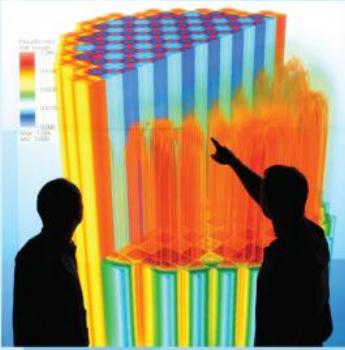




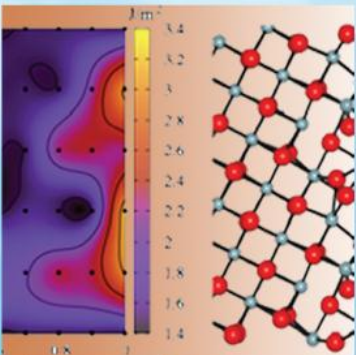
Power uprates  
and plant life extension



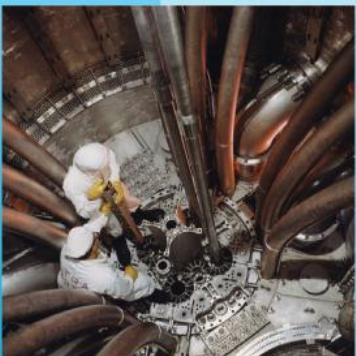
Engineering design  
and analysis



Science-enabling  
high performance  
computing



Fundamental science



Plant operational data

**L3:VUQ.SAUQ.P2-2.01**  
**Brian Williams**  
**LANL**  
**Completed: 4/25/11**



U.S. DEPARTMENT OF  
**ENERGY**

**Nuclear Energy**

LA-UR-

*Approved for public release;  
distribution is unlimited.*

*Title:*

*Author(s):*

*Intended for:*



Los Alamos National Laboratory, an affirmative action/equal opportunity employer, is operated by the Los Alamos National Security, LLC for the National Nuclear Security Administration of the U.S. Department of Energy under contract DE-AC52-06NA25396. By acceptance of this article, the publisher recognizes that the U.S. Government retains a nonexclusive, royalty-free license to publish or reproduce the published form of this contribution, or to allow others to do so, for U.S. Government purposes. Los Alamos National Laboratory requests that the publisher identify this article as work performed under the auspices of the U.S. Department of Energy. Los Alamos National Laboratory strongly supports academic freedom and a researcher's right to publish; as an institution, however, the Laboratory does not endorse the viewpoint of a publication or guarantee its technical correctness.

# Demonstration of Validation Methodology Applied to VIPRE-W Boiling Index Calculations

Brian J. Williams, Brian M. Adams, Yixing Sung, Walter R. Witkowski

## 1. Introduction

The initial CASL validation plan (AMA.VAL.Y1.02) provided a roadmap for validating the Virtual Environment for Reactor Applications (VERA) software for industrial applications. The general approach was adapted to several CASL challenge problems, including Crud Induced Power Shift (CIPS). In this demonstration supporting CASL milestone VUQ.SAUQ.Y1-2.01, we are concerned with comparing VIPRE-W calculations of boiling index with experimental calculations of crud index.

A component of the initial VERA release, VIPRE-W is a Westinghouse version of the VIPRE-01 code. VIPRE-01 is a thermal hydraulic subchannel code based on the COBRA codes developed by Pacific Northwest National Laboratories under sponsorship of the Electric Power Research Institute (EPRI) [1]. VIPRE-W contains enhancements for pressurized water reactor applications, including the mass evaporation and grid spacer heat transfer models required for CIPS risk assessment.

Figure 1 shows an axial diagram of a Westinghouse fuel assembly in Plant B that had a CIPS occurrence. For specified settings of uncertain physics model parameters, VIPRE-W calculates a boiling index in each of the axial regions 4A, 4B, 5A, 5B, 6A, 6B, 7A, and 7B. The grid span for each axial region consists of 5-7 nodes, each with four channels in the VIPRE-W model. For each node, the percentage of channels in subcooled boiling (positive mass evaporation rate) is calculated. The boiling index for each axial region is then computed as a weighted average of these percentages across its constituent nodes, with weights given by the lengths of each node. Additional details on the VIPRE-W simulations used in this study are provided in [2].

Experimental measurements of crud index for four assemblies belonging to Plant B are used to calibrate uncertain parameters in VIPRE-W physics models and to validate VIPRE-W predictions of boiling index. Crud index was estimated for each axial region 4A-7B by observing the relative surface area covered with crud [3]. Crud index measurements from three assemblies designated F71, F22, and F88 were used for parameter calibration. Crud index data from assembly F09 were held aside and compared with calibrated VIPRE-W predictions of F09 boiling indices for each axial region.

It is critical to note that VIPRE-W boiling index is indirectly related to crud formation and thus should be cautiously compared to observed crud index. A key assumption in the study is that the VIPRE-W boiling index is comparable to the crud index. Future studies with VERA capable of predicting crud deposition will allow direct calculation of crud index, allowing a scientifically defensible validation

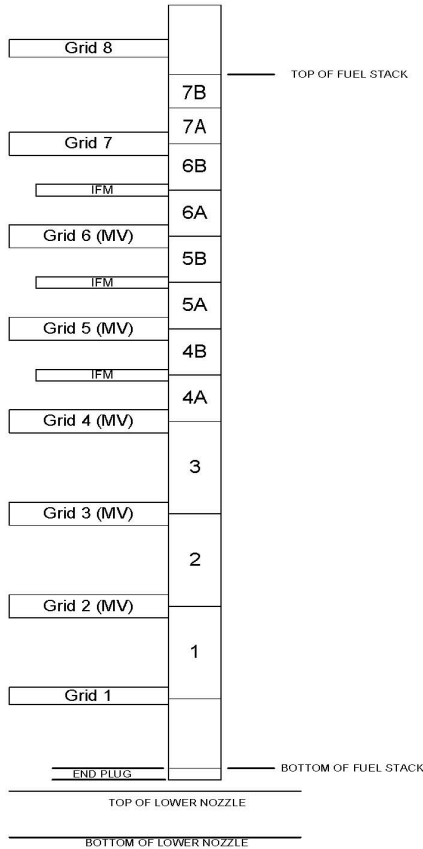


Figure 1. Diagram of fuel rod in Plant B assemblies showing axial regions 4A – 7B in which VIPRE-W calculated boiling index is compared with experimental crud index.

utilizing the approach outlined in the next section.

Table 1 provides the five uncertain physics (or modeling) parameters with their allowable ranges of variation in VIPRE-W calculations. These parameters are assigned uniform prior distributions on these ranges in the sensitivity analyses and calibrations of the next section.

Table 1. VIPRE-W uncertain physics parameters and allowable ranges.

Parameter	Range	Parameter	Range
Lead coefficient of Dittus-Bolter Correlation (DBCoeff)	0.019 – 0.033	Lateral Resistance Correlation Coefficient (LRCCoeff)	1.5 - 4
Lead Coefficient of Grid Heat Transfer Model (GHTCoeff)	2 - 6	Exponent of Partial Boiling Model (ExpPBM)	1 - 4
Axial Friction Correlation Coefficient (AFCCoeff)	0.1 – 0.25		

Table 2 presents the experimentally observed values of crud index for each axial region across the four assemblies. Observational uncertainties were not recorded; however, they are a required component in statistical calibration of uncertain model parameters. For the purposes of this analysis, we assumed a binomial model for uncertainty in crud index, having one standard deviation equal to 10% of a crud index measurement of 0.5 (ie., 0.05). Future applications of these data for VERA validation will explore the sensitivity of results to assumptions about observation error.

Table 2. Crud index measurements for four Plant B assemblies used in calibration and validation analyses.

Axial Region	F71	F22	F88	F09
7B	0.025	0.025	0.35	0.325
7A	0.1075	0.0375	0.4625	0.3
6B	0.475	0.2125	0.7875	0.4125
6A	0.38	0.1375	0.625	0.35
5B	0.3925	0.125	0.5625	0.35
5A	0.2125	0.075	0.3375	0.2375
4B	0.1175	0.0375	0.2125	0.1625
4A	0.0175	0.0125	0.095	0.05

## 2. Analyses

For each assembly, VIPRE-W boiling index output is viewed as a function of axial location. A symmetric Latin hypercube design [4] in the five physics variables of Table 1 was used to specify 200 VIPRE-W runs, from which surrogate models of boiling index were built for each assembly. These surrogate models were utilized for all sensitivity analyses and calibrations of the physics variables described in this section.

We provide a brief description of the statistical modeling approach taken in this study to provide context for the results presented. Let  $\boldsymbol{\eta}(\mathbf{t})$  denote the vector of boiling indices calculated at each of the eight axial regions 4A – 7B, corresponding to physics variable setting  $\mathbf{t}$ . An orthogonal basis representation for boiling index is specified,

$$\boldsymbol{\eta}(\mathbf{t}) = \mathbf{k}_1 w_1(\mathbf{t}) + \cdots + \mathbf{k}_{p_\eta} w_{p_\eta}(\mathbf{t}).$$

The basis vectors  $\mathbf{k}_1, \dots, \mathbf{k}_{p_\eta}$  are eigenvectors of the principal component decomposition derived from the covariance matrix of the 200 VIPRE-W calculations of boiling index, while all principal component coefficients  $w_i(\mathbf{t})$  are modeled as independent Gaussian processes [5,6]. All components having positive variance are included in this surrogate model.

For each assembly, the sensitivity of boiling index to variation in the five physics variables was assessed using the methodology [7], extended to account for uncertainty in the surrogate models [8]. Table 3 provides main and total effect indices [9] for each physics variable by assembly. Assuming a uniform distribution on the inputs, the main effect index for a specific input measures the fraction of total output variance explained by variation in that input. The total effect index measures the fraction of total output variance explained by the single and all interaction effects involving that input. The results in Table 3 show that output variance is dominated by variation in DBCoeff (explaining roughly 95% of total output variance), and that interaction effects involving multiple inputs are fairly insignificant. Therefore, the crud index measurements will inform mostly on DBCoeff, providing a focus for the following calibration results.

Table 3. Sensitivity analysis results for VIPRE-W boiling index across four Plant B assemblies (ME = main effect; TE = total effect).

	F71		F22		F88		F09	
Parameter	ME (%)	TE (%)						
DBCoeff	94.8	98.1	93.6	98.1	93.1	96.8	96.6	98.4
GHTCoeff	1.7	4.8	0.4	3.3	2.5	5.6	1.2	2.8
AFCCoeff	0	0.4	0.2	3.2	0.4	1.6	0.3	0.7
LRCCoeff	0	0.4	0.1	2.8	0	0.6	0	0.2
ExpPBM	0	0.3	0.1	2.8	0	0.4	0	0.2

Let  $\boldsymbol{\theta}$  denote the unknown, best values of the five physics parameters given in Table 1. By “best,” we seek an answer to the question, “What probability distribution for  $\boldsymbol{\theta}$  is most consistent with experimental evidence and prior information?” The approach taken in this analysis is fully Bayesian. As mentioned previously, we assume a uniform prior distribution on  $\boldsymbol{\theta}$  with ranges given in Table 1. In general, expert judgment or small-scale data may be used to inject additional prior information.

Although the true crud index  $\zeta$  is unobservable, it is related to the experimental values  $\mathbf{y}$  through an observational error model  $\boldsymbol{\varepsilon}$ ,  $\mathbf{y} = \boldsymbol{\zeta} + \boldsymbol{\varepsilon}$ . The error model is stochastic and represents the investigator's assumptions on the underlying random processes leading to replicate variation in experimental results. This includes measurement errors but extends beyond those to incorporate inherently irreducible (aleatory) uncertainties. We assume independent Gaussian errors across each element  $y_i$  of the crud index vector  $\mathbf{y}$ , having binomial variances  $y_i(1 - y_i)/100$ .

The "best" VIPRE-W boiling index calculation is connected to the true crud index through a refinement of the above observational error model:  $\boldsymbol{\zeta} = \boldsymbol{\eta}(\boldsymbol{\theta}) + \boldsymbol{\delta}$ . The statistical model for  $\boldsymbol{\eta}$  introduced earlier is retained, and discrepancy  $\boldsymbol{\delta}$  is modeled as a kernel regression:  $\boldsymbol{\delta} = \mathbf{D}\mathbf{v}$ , where the columns of  $\mathbf{D}$  are 13 Gaussian kernels centered on a set of equally spaced knots spread out along the axial dimension of the fuel rod and  $\mathbf{v}$  are *a priori* statistically independent Gaussian random variables. Discrepancy accounts for the possibility that no best setting  $\boldsymbol{\theta}$  can be found such that the resulting VIPRE-W boiling indices match the corresponding experimental crud indices simultaneously to within observational error.

With these specifications, calibration proceeds by solving an inverse problem for  $\boldsymbol{\theta}$  to obtain its posterior distribution [10-12]. This is often accomplished through forward sampling algorithms such as Markov chain Monte Carlo (the method adopted in this analysis) although recently adjoint methods have been employed [13]. Additional details on calibration of  $\boldsymbol{\theta}$  in the presence of functional output (as is the case here) can be found in [14]. Calibrated predictions of boiling index are obtained by propagating a posterior sample of  $\boldsymbol{\theta}$  forward through VIPRE-W. Such predictions are used in the validation assessment for the F09 assembly described below.

Two joint calibrations of the five physics inputs  $\boldsymbol{\theta}$  were performed, the first to crud index data from F71 and F22 simultaneously, and the second to crud index data from F71, F22, and F88 simultaneously (see Table 2). The crud indices from different assemblies are taken to be conditionally independent given a value for  $\boldsymbol{\theta}$ . Figure 2 compares calibrated VIPRE-W boiling indices from these two analyses for the F22 and F88 assemblies. Two immediate conclusions arise:

- The two joint calibrations do not result in predictions that are entirely consistent. This can be seen, for example, in the central axial regions 5B, 6A, and 6B. This is a consequence of the fact that the average power for the three assemblies differs: 1.18 times nominal (F71), 1.26 (F22), and 1.29 (F88). Including the higher power assembly F88 in the joint calibration modifies the calibration sufficiently to cause a shift in the resulting predictions at some axial locations. This effect is clearly seen in Figure 3, which shows the marginal posterior distribution for the most sensitive physics input DBCoeff arising from both calibrations. Inclusion of F88 causes a shift to larger values of DBCoeff, suggesting the undesirable result that physics variable calibration depends significantly on operating conditions.

- Significant discrepancy between observed crud index and calibrated VIPRE-W boiling index exists at some axial locations.

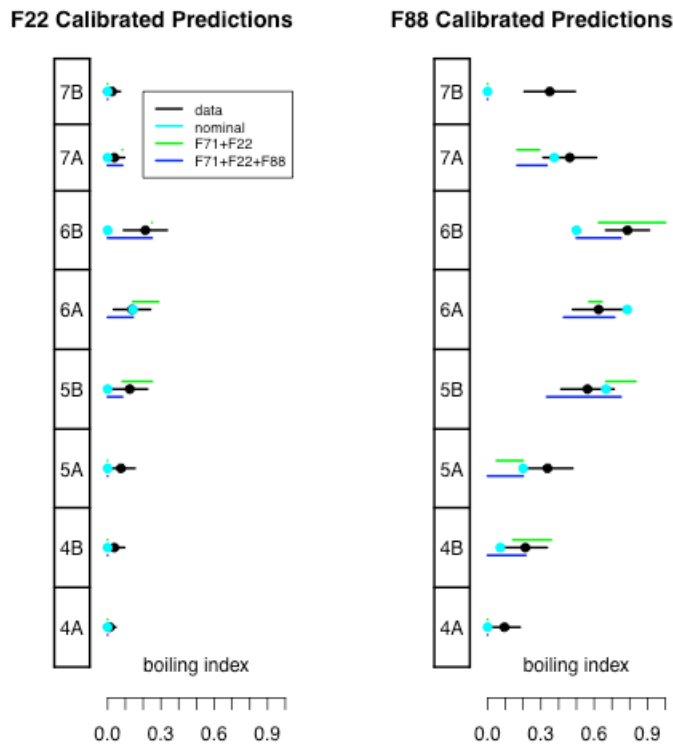


Figure 2. Calibrated VIPRE-W boiling index predictions for assemblies F22 (left) and F88 (right). Results are given for the nominal VIPRE-W boiling index calculation (cyan) and two calibrations using crud index data (black) from F71 and F22 (green) and F71, F22, and F88 (blue). 95% prediction intervals are shown for the calibrated predictions along with three-sigma bounds on the observation errors.

Calibrated predictions of VIPRE-W boiling index for F09 were computed and shown in Figure 4 for the two calibrations described previously. The purpose of examining these predictions is to assess if comparing them with the corresponding F09 crud index measurements allows for validation of VIPRE-W boiling index calculations for this assembly. As with assessment of the calibration results above, although the crud index measurements from the other assemblies substantially constrain VIPRE-W predictions of F09 boiling index, significant discrepancy remains at several axial locations. Furthermore, inclusion of F88 crud index measurements in the calibration generally improves VIPRE-W predictions of F09 boiling index at axial locations 5B, 6A and 6B. This is not surprising given the average power of the F09 assembly is the same as that of F88; nevertheless, uncertainties in VIPRE-W predictions at these axial locations are large relative to observational uncertainty and would be reduced simultaneously with the mitigation of discrepancy that is anticipated with access to the enhanced capabilities of VERA.

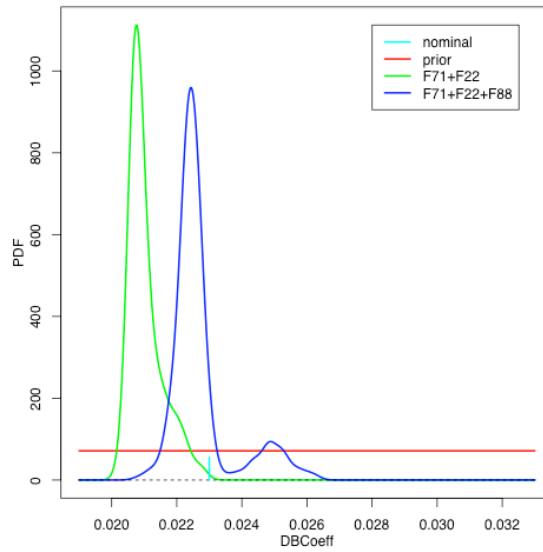


Figure 3. Prior (red) and marginal posterior distributions for DBCoeff based on two calibrations to crud index from F71 and F22 (green) and F71, F22, and F88 (blue).

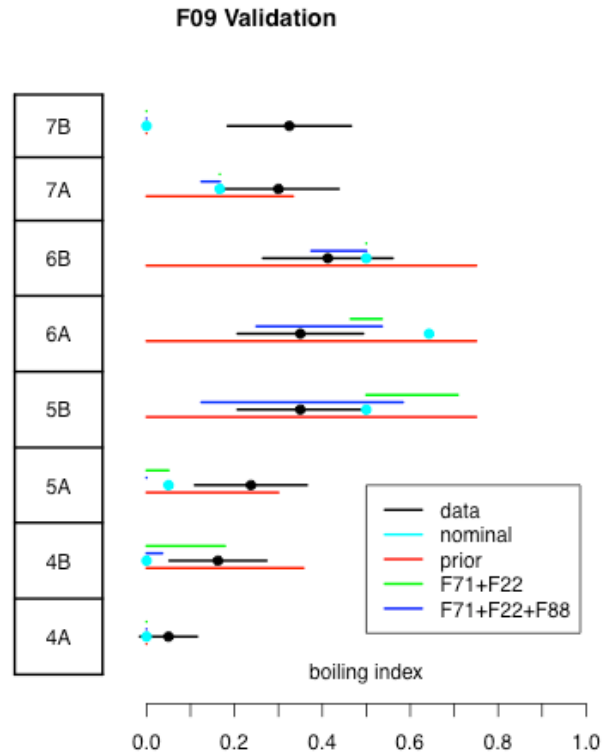


Figure 4. Calibrated VIPRE-W boiling index predictions for assembly F09. Results are given for the nominal VIPRE-W boiling index calculation (cyan) and two calibrations using crud index data (black) from F71 and F22 (green) and F71, F22, and F88 (blue). 95% prediction intervals are shown for the calibrated predictions along with three-sigma bounds on the observation errors.

Table 4 presents the nominal values for the five uncertain physics variables and their posterior median values from the calibration to the F71, F22, and F88 crud index measurements.

Table 4. Nominal and posterior median values for uncertain physics variables.

Parameter	Posterior Median	Nominal	Parameter	Posterior Median	Nominal
DBCoeff	0.0225	0.023	LRCCoeff	3.008	2.66
GHTCoeff	4.444	2.22	ExpPBM	2.985	2
AFCCoeff	0.203	0.184			

Table 5 compares the VIPRE-W boiling index predictions for F09 at axial levels 4A – 7B resulting from the posterior median values in Table 4 with those from the nominal values and the observed crud index values. The only differences in the predictions from the posterior median and nominal values occur in axial regions 6A, where the F09 crud index is substantially over-predicted by the nominal values, and 5A where the nominal prediction is slightly closer to the observed data.

Table 5. Comparison of VIPRE-W boiling index predictions for F09 using the posterior median and nominal parameter values.

	Axial Location							
	4A	4B	5A	5B	6A	6B	7A	7B
Posterior Median	0	0	0	0.5	0.5	0.5	0.167	0
Nominal	0	0	0.05	0.5	0.643	0.5	0.167	0
F09 Crud Index	0.05	0.1625	0.2375	0.35	0.35	0.4125	0.3	0.325

This study included four uncertain operating parameters that were fixed at nominal values for the calibration studies above. Table 6 lists these parameters with their ranges and the means and standard deviations of independent Gaussian distributions (truncated on the given ranges) representing uncertainty in their values. Figure 5 presents VIPRE-W boiling index predictions for assembly F09 that includes these uncertainties in addition to the physics uncertainties. It is clearly seen that inclusion of operating parameter uncertainty substantially increases uncertainty in VIPRE-W boiling index predictions beyond the level seen in Figure 4.

Table 6. Operating parameters with ranges and means and standard deviations of Gaussian distributions (truncated) representing their uncertainty.

Parameter	Ranges	Mean	Standard Deviation
Assembly Power (power)	60.9 – 73.0	66.9454	2.008362
Coolant Flow (flow, gpm)	16.05 – 16.88	16.47	0.2058323
Temperature (temperature, °F)	554.4 – 566.4	558.8	3
System Pressure (pressure, psia)	2185 - 2315	2270	25

Therefore, validation of VERA crud index predictions will require substantial reduction in operating parameter uncertainty.

### 3. Future work

This calibration/validation study is limited by the fact that VIPRE-W alone cannot calculate crud index; rather, it computes boiling index as a surrogate. This will be remedied with the next release of VERA, which includes the BOA code for computing crud deposition. The interpretability of results from this or similar studies is expected to improve with the VERA multi-physics codes, allowing better comparisons between code calculations and experimental data. Furthermore, the following extensions to the methodology in this study will be pursued in future iterations subject to feasibility:

- Inclusion of small-scale data to calibrate separate physics models within VERA component codes ANC, VIPRE-W and BOA.
- Inclusion of additional plant data for calibration and validation of separate and coupled physics models relevant to prediction of crud deposition.
- Application of rigorous quantitative validation criteria (eg. [15]).
- Replacement of statistical surrogates with direct code calculations in sensitivity analysis and calibration algorithms for applications in which code calculations are relatively fast (on the order of minutes).
- Comparison of results with alternative calibration and validation paradigms.

### F09 Validation with Operating Uncertainty

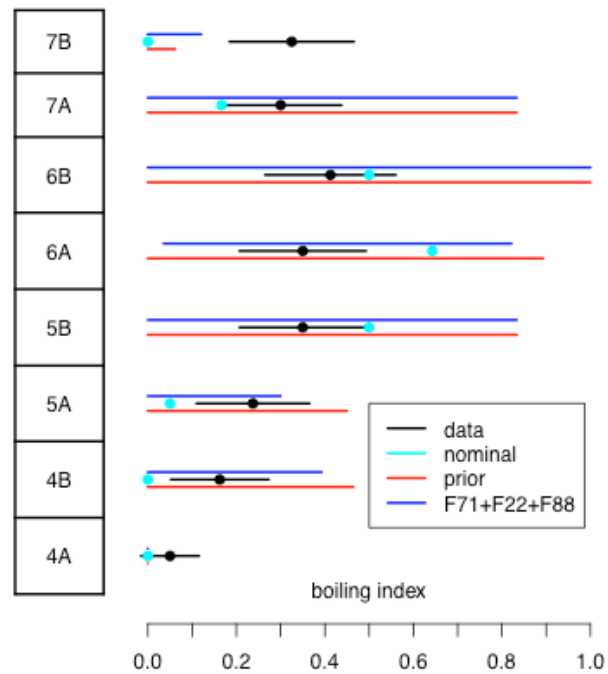


Figure 5. VIPRE-W boiling index predictions for assembly F09, including operating and physics parameter uncertainties. Results are given for the nominal VIPRE-W boiling index calculation (cyan), prior uncertainty in the physics variables (red), and physics uncertainty resulting from the calibration to crud index data (black) from F71, F22, and F88 (blue). 95% prediction intervals are shown for the predictions along with three-sigma bounds on the observation errors.

- Extension to additional CASL challenge problems.

## References

1. Stewart, C.W., Cuta, J.M., Montgomery, S.D., Kelly, J.M., Basehore, K.L., George, T.L., Rowe, D.S., VIPRE-01: A thermal-hydraulic code for reactor cores, Volumes 1—3 (Revision 3, August 1989) and Volume 4 (April 1987), NP-2511-CCM-A, Electric Power Research Institute.
2. Adams, B.M., Witkowski, W.R., Sung, Y., CASL L2 Milestone Report: VUQ.Y1.03, "Enable Statistical Sensitivity and UQ Demonstrations for VERA," SAND2011-2238, Sandia National Laboratories.
3. Sabol, G.P., Secker, J.R., Kormuth, J., Kunishi, H., Nuhfer, D.L., Rootcause investigation of axial power offset anomaly, TR-108320, Electric Power Research Institute, June 1997.

4. Ye, K.Q., Li, W., Sudjianto, A., Algorithmic construction of optimal symmetric Latin hypercube designs, *Journal of Statistical Planning and Inference* 90 (2000), pp. 145-159.
5. Sacks, J., Welch, W.J., Mitchell, T.J., Wynn, H.P., Design and analysis of computer experiments (with discussion), *Statistical Science* 4 (1989), pp. 409-423.
6. Santner, T.J., Williams, B.J., Notz, W.I., *Design and Analysis of Computer Experiments*, Springer, 2003.
7. Lamboni, M., Monod, H., Makowski, D., Multivariate sensitivity analysis to measure global contribution of input factors in dynamic models, *Reliability Engineering and System Safety* 96 (2011), pp. 450-459.
8. Oakley, J.E., O'Hagan, A., Probabilistic sensitivity analysis of complex models: a Bayesian approach, *Journal of the Royal Statistical Society, Series B* 66 (2004), pp. 751-769.
9. Saltelli, A., Chan, K., Scott, E.M., *Sensitivity Analysis*, John Wiley & Sons, 2000.
10. Kennedy, M., O'Hagan, A., Bayesian calibration of computer models (with discussion), *Journal of the Royal Statistical Society, Series B* 63 (2001), pp. 425-464.
11. Higdon, D., Kennedy, M., Cavendish, J., Cafoe, J., Ryne, R.D., Combining field observations and simulations for calibration and prediction, *SIAM Journal on Scientific Computing* 26 (2004), pp. 448-466.
12. Williams, B., Higdon, D., Gattiker, J., Moore, L., McKay, M., Keller-McNulty, S., Combining experimental data and computer simulations, with an application to flyer plate experiments, *Bayesian Analysis* 1 (2006), pp. 765-792.
13. Cacuci, D.G., Ionescu-Bujor, M., Best-estimate model calibration and prediction through experimental data assimilation – I: Mathematical framework, *Nuclear Science and Engineering* 165 (2010), pp. 18-44.
14. Higdon, D., Gattiker, J., Williams, B., Rightley, M., Computer model calibration using high-dimensional output, *Journal of the American Statistical Association* 103 (2008), pp. 570-583.
15. Wang, S., Chen, W., Tsui, K.-L., Bayesian validation of computer models, *Technometrics* 51 (2009), pp. 439-451.